

# Test of Silicon Sensors for a High Rate Pixel Detector for the NA62 Experiment

February 6, 2008

M. Fiorini<sup>a</sup>, F. Osmic<sup>b</sup>, F. Petrucci<sup>a</sup>, P. Riedler<sup>b</sup>

<sup>a</sup>Dipartimento di Fisica dell'Università and Sezione INFN, 44100 Ferrara, Italy

<sup>b</sup>CERN, CH-1211 Geneva 23, Switzerland

## Abstract

The NA62 experiment proposes to study the very rare Kaon decay  $K^+ \rightarrow \pi^+ \nu \bar{\nu}$  at the CERN SPS. In order to track the high intensity Kaon beam before its decay a set of three high precision silicon pixel detector planes has been proposed (GigaTracKer – GTK). In the current layout three hybrid silicon pixel detector layers will be operated in a high fluence environment (up to  $2 \times 10^{14}$  1MeV  $n_{eq}/cm^2$ ) and provide precise tracking and timing information. A study to evaluate the effects of particle radiation on the sensor performance has been carried out using prototype diodes. The results of this study are presented and possible operation parameters are discussed.

## 1 Introduction

The three GTK stations will provide a momentum and angular track measurement of the initial Kaon beam and allow tracking of the Kaons up to the decay region. The GTK will also be the first pixel detector that will provide high precision timing ( $\sigma_t \sim 160$  ps/track) information that can be used to generate a tight Kaon-pion time coincidence with a fast hodoscope [1].

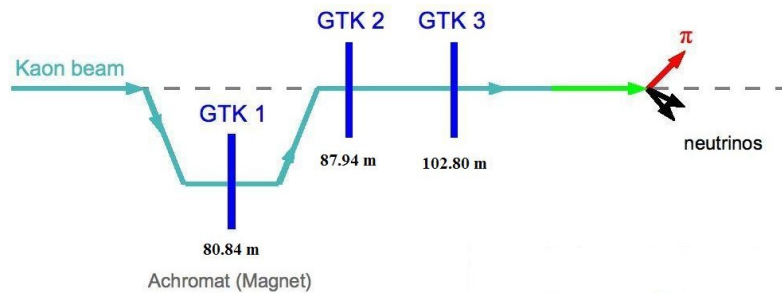


Figure 1: Schematic of the three GTK stations in the Kaon beam.

### 1.1 Layout of the GTK Planes

The current design foresees the use of hybrid pixel detectors for the GTK planes. Hybrid pixel detectors have been developed for all LHC experiments and provide the possibility to separately optimize readout electronics and sensors. Figure 2 shows a schematic drawing of one GTK plane. Each plane consists of one silicon pixel sensor connected to 2 x 5 pixel chips. Outside the beam area multilayer cables and SMD components will be mounted for connection of the pixel chips with the off-detector electronics.

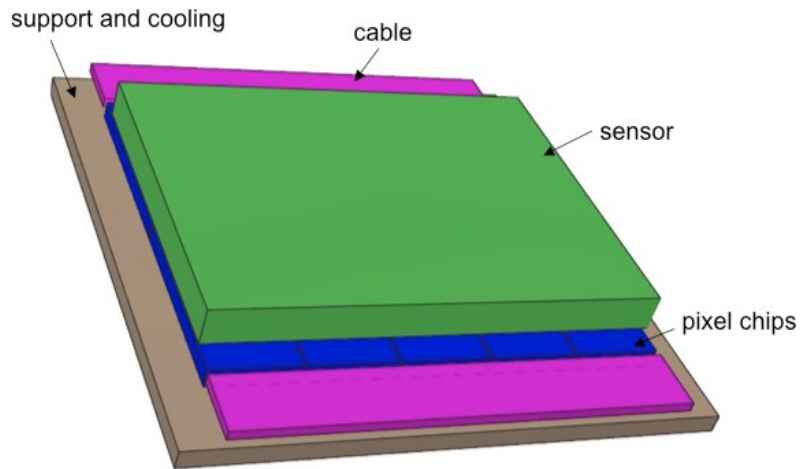


Figure 2: Schematic view of one GTK plane.

In the current design the dimensions of the silicon sensor have been fixed to 27 mm x 60 mm to cover the full beam area. The size of the active area of the readout chip is approximately 13.5 mm x 12 mm with a matrix of 45 x 40 pixels of 300  $\mu\text{m}$  x 300  $\mu\text{m}$ . The pixel chips are connected in two rows to the sensor as shown in Figure 3. In order to cover the space between individual readout chips elongated pixel cells ( $\sim 450\mu\text{m}$  instead of 300 $\mu\text{m}$ ) will be used in the inter-chip regions.

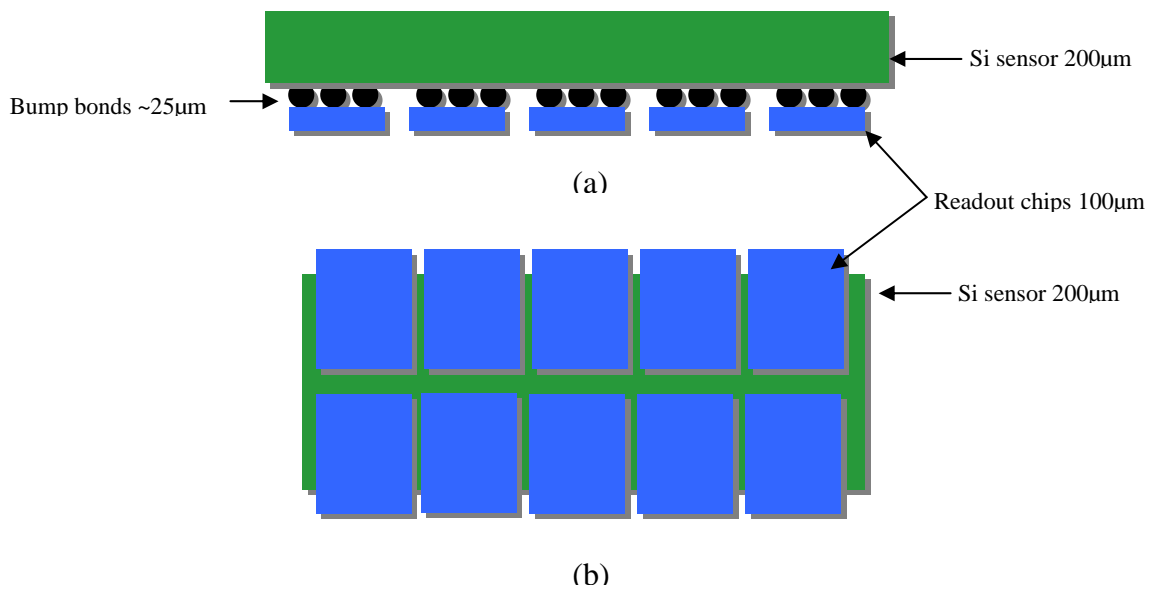


Figure 3: Schematic sketch of one GTK plane: (a) side view, (b) top view showing the positions of the readout chips on top of the sensor.

The material budget limitations are one of the major challenges for the GTK. The design layout foresees a total material budget of maximum 0.5%  $X_0$  per station in order to minimize the multiple scattering before the decay region.

To comply with the material budget requests the sensor thickness will be limited to 200  $\mu\text{m}$ . This results in a mean signal of 19.000 e-h pairs for a 75 GeV/c Kaon beam [2, 3]. Even though thinner sensors would be beneficial to the overall material budget, the loss in signal would reduce the timing performance of the plane and would also result in a lower production yield. To reduce the material in the beam a target thickness of the readout chips of 100  $\mu\text{m}$  has been set. Previous experiences with pixel detectors with similar material budget limitations have resulted in chip thicknesses of 150  $\mu\text{m}$  for the module production [4].

The operating environment and low mass of the detector will require efficient cooling in order to keep the radiation induced leakage current at an acceptable value for stable operation. A target operation temperature of  $\leq 5^\circ\text{C}$  has been proposed to maximize the operating time in the beam limited by radiation induced leakage current. A further requirement for the operation is that the GTK planes will be mounted inside the vacuum beam pipe to avoid additional material in the beam path, e.g. vacuum windows.

In the current proposed layout the material inside the beam area will consist only of the sensor, the readout chips and the bump bonding and the carbon fibre support for cooling. Mechanical support structures, SMD components and multilayer cables will be placed outside the beam area. In Table 1 the materials inside the beam area and the equivalent radiation lengths are listed.

Component	Material	Thickness [ $\mu\text{m}$ ]	$X_0$ [%]
Sensor	Si	200	0.21
Bump Bonds*	Pb-Sn	~25	0.001
Readout Chip	Si	100	0.11
Carbon Fibre	C	100	0.05

Table 1: Materials and thicknesses orthogonal to beam direction (\* assuming 60% Sn and 40% Pb with bump diameters of 25 $\mu\text{m}$  smeared over full sensor surface of 27 mm x 60 mm).

## 1.2 Operating Conditions

In order to achieve the desired time resolution an over-depleted operation of the detector is required. From the electronics requirements a total charge collection time of less than ~6 ns is required which can be achieved with an over-depletion voltage of at least ~200V [5]. This results in requirements in the design of the sensors to allow for high voltage operation, i.e. to ensure current stability.

The NA62 experiment will be operated in a high intensity beam line at the SPS. The number of incident particles on one GTK plane per day is foreseen to reach up to  $\sim 2 \times 10^{12}$  particles/cm<sup>2</sup> in the hot center of the beam. In the outer regions of the beam covering the GTK planes a particle rate of  $\sim 7 \times 10^{11}$ /cm<sup>2</sup>/day are expected. Assuming a yearly run time of 100 days the maximum fluence of particles in the hot center of the planes will amount up to  $2 \times 10^{14}$  particles/cm<sup>2</sup>. Using a damage factor of 0.37 to convert the Kaon-pion beam fluence to the 1MeV neutron equivalent and using a safety factor of 2 results in a maximum fluence of  $\sim 2 \times 10^{14}$  1MeV  $n_{\text{eq}}$ /cm<sup>2</sup> over a 100 day run period in the hot center of the planes. This fluence is comparable to the estimated fluence foreseen during a 10 year operation of the silicon trackers of ATLAS or CMS.

In Table 2 the main characteristics of one GTK plane are summarized:

<b>Sensor thickness</b>	200 $\mu\text{m}$
<b>Pixel size</b>	300 $\mu\text{m}$ x 300 $\mu\text{m}$ (elongated pixels on chip borders)
<b>Sensor size</b>	27 mm x 60 mm
<b>Readout chips</b>	13.5 mm x 12 mm (active area)
<b>Module</b>	1 sensor and 10 readout chips
<b>V<sub>op</sub></b>	$>V_{fd}+200\text{V}$
<b>Environment</b>	vacuum
<b>Requested operation time</b>	100 days
<b>Operating temperature</b>	$\leq 5^{\circ}\text{C}$

*Table 2: Main characteristics of the operating conditions of the GTK planes.*

In order to study the effects of radiation damage on the silicon sensor properties a series of prototype diodes was irradiated to different fluences. In the following section the samples and the irradiations that have been carried out are presented.

## 2 Irradiation Tests

Prototype p-in-n diodes were produced on high resistivity Float Zone (FZ) wafers (resistivity  $\sim 6 \text{ k}\Omega\text{cm}$ ) in order to study the radiation effects at different fluences and to allow to measure signal characteristics of the irradiated diodes with an infrared laser setup. All diodes were produced by ITC-IRST<sup>1</sup> on 200  $\mu\text{m}$  thick wafers. Two different guard ring designs were used, either 4 or 12 guard rings surrounding the pad.

The diodes were diced and mounted on small PCBs to be able to irradiate the diodes under bias. During irradiation all diodes were biased at 30V. Figure 4 shows a picture of one diode prepared for irradiation and mounted inside a Plexiglas transport box.

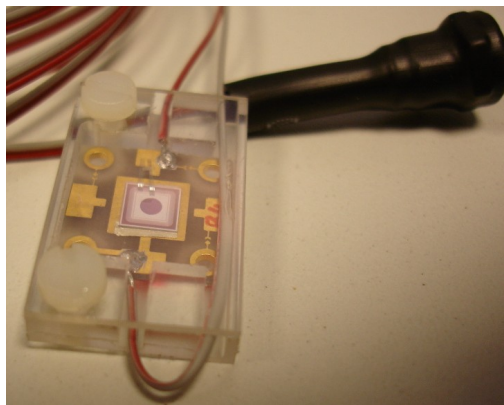


*Figure 4: One prototype diode mounted on a PCB inside the Plexiglas transport box. The opening in the Aluminium in the center of the pad is used for laser measurements.*

<sup>1</sup> ITC- IRST, I-38050 Povo (Trento), Italy

Three irradiations were carried out using 24 GeV/c protons at the CERN PS (August 2006) and high energetic neutrons in the TRIGA reactor in Ljubljana (December 2005 and February 2007). In total 16 diodes were irradiated to various fluences between  $1 \times 10^{12}$   $1\text{MeV } n_{\text{eq}} \text{ cm}^{-2}$  and  $2 \times 10^{14}$   $1\text{MeV } n_{\text{eq}}/\text{cm}^2$ . Table 3 lists all irradiated diodes indicating the pad size and the fluences to which they have been irradiated to.

Diode	Pad area [mm <sup>2</sup> ]	Irradiation facility	Particles	Fluence [1MeV $n_{\text{eq}}/\text{cm}^2$ ]
A1	7×7	Ljubljana	neutrons	$2.0 \times 10^{14}$
A2	7×7	Ljubljana	neutrons	$3.0 \times 10^{13}$
B1	3×3	Ljubljana	neutrons	$2.0 \times 10^{14}$
B2	3×3	Ljubljana	neutrons	$1.0 \times 10^{12}$
B3	3×3	Ljubljana	neutrons	$2.0 \times 10^{12}$
B4	3×3	Ljubljana	neutrons	$1.0 \times 10^{13}$
846	3×3	CERN PS	protons	$3.49 \times 10^{12}$
847	3×3	CERN PS	protons	$5.92 \times 10^{12}$
848	3×3	CERN PS	protons	$8.40 \times 10^{12}$
849	7×7	CERN PS	protons	$2.51 \times 10^{13}$
B10	3×3	Ljubljana	neutrons	$1.5 \times 10^{12}$
B11	3×3	Ljubljana	neutrons	$3.0 \times 10^{12}$
B12	3×3	Ljubljana	neutrons	$5.0 \times 10^{12}$
B13	3×3	Ljubljana	neutrons	$7.0 \times 10^{12}$
B14	3×3	Ljubljana	neutrons	$1.5 \times 10^{13}$
B15	3×3	Ljubljana	neutrons	$1.0 \times 10^{14}$

Table 3: List of irradiated diodes.

The diode B1 was damaged during mounting and therefore the data of this diode are not considered. The corresponding fluence was covered by another diode, namely A1. Figure 5 shows the estimated fluence levels for the average radiation dose expected as function of the run time. The diodes that have been irradiated to the equivalent fluences are indicated in the graph.

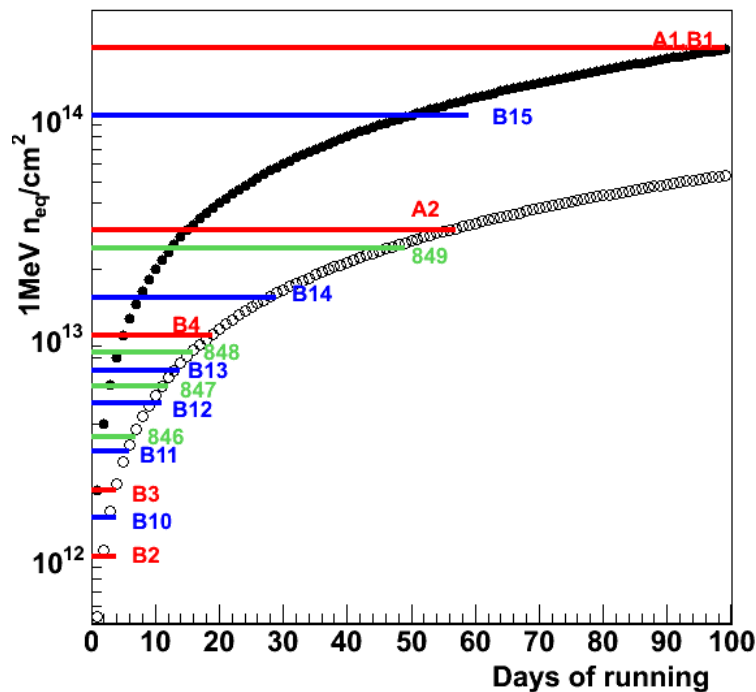


Figure 5: Estimated fluence levels for different days of running for the average radiation level and the hot center. The diodes irradiated to the equivalent fluence levels are indicated in the plot.

## 2.1 CV-IV Measurement Setup

All diodes have been tested prior and after irradiation using a C-V/I-V test setup at CERN. The capacitance-voltage and current-voltage characteristics have been measured using an HP4284 LCR-meter and two Keithley 2410 source meters.

Post irradiation measurements were carried out in the same facility which also provides an air-convection oven with precise temperature control. After irradiation all diodes were annealed in several time steps at 80°C up to a maximum time of 100 minutes [6] and C-V/I-V measurements were carried out at every annealing step.

The capacitance  $C$  of the diode is inversely proportional to the depletion depth which itself is directly proportional to the square of the applied bias voltage  $V$ :

$$\frac{1}{C^2} \propto V \quad \text{Eq. 1}$$

Figure 6 shows a C-V measured on diode B13 and plotted as  $1/C^2$  vs  $V$  to determine the full depletion voltage. The capacitance of the diode decreases with increasing bias voltage until full depletion ( $V_{fd}$ ) is reached and then remains constant. Graphically,  $V_{fd}$  has been determined for all diodes by plotting  $1/C^2$  versus  $V_{bias}$  and fitting lines to the two regions as shown in Figure 6. The intersection of the lines determines  $V_{fd}$ .

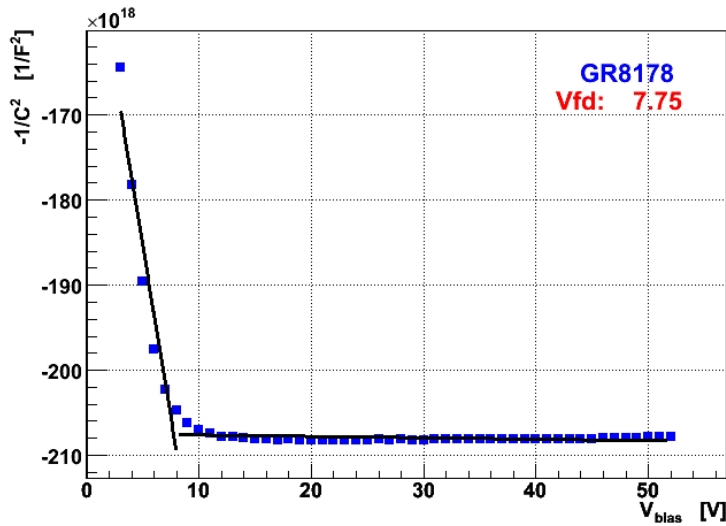


Figure 6: Dependence of the capacitance on the bias voltage for diode B13. Fit with two straight lines in order to extract the full depletion voltage, which amounts to  $V_{fd} = (7.8 \pm 1.0)$  V.

For the capacitance measurements frequencies between 500 Hz and 10 kHz were chosen. Even though before irradiation no significant difference depending on the frequency is observed, the radiation induced defects in the bulk and oxide influence the C-V characteristic after irradiation [7]. Therefore the measurements after irradiation were carried out at two different frequencies at least, and in most cases at three frequencies (1 kHz, 5 kHz, 10 kHz). Figure 7 shows a C-V measurement carried out on diode B15 at three different frequencies (1 kHz, 5 kHz and 10 kHz).

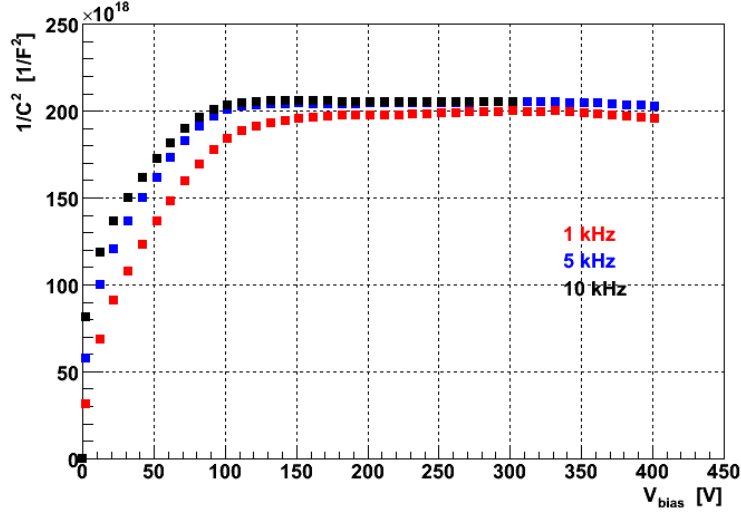


Figure 7: C-V characteristic of the diode B15 measured at three different frequencies.

Leakage currents of pad and guard rings as function of the bias voltage were measured at temperatures of about 20-25°C ( $T_{meas}$ ). All measurements were normalized to 20°C or other temperatures (T) using the following relation:

$$I(T) = I(T_{meas}) \times \left( \frac{273.2+T}{273.2+T_{meas}} \right)^{\frac{3}{2}} \times e^{\frac{E}{k} \left( \frac{1}{273.2+T_{meas}} - \frac{1}{273.2+T} \right)} \quad \text{Eq. 2}$$

where  $E=1.12$  eV is the band gap energy and  $k=8.617 \times 10^{-5}$  eV/K is the Boltzmann constant.

The I-V characteristics of all diodes have been measured up to at least 200V, in some cases also to higher voltages. The temperatures during the measurements were recorded using a Pt1000 sensor mounted on the measurement chuck. All currents have been corrected to the temperatures indicated in the graphs.

Figure 8 shows an I-V characteristic measured on one diode after irradiation and annealing up to 1000V to test the high voltage current behaviour.

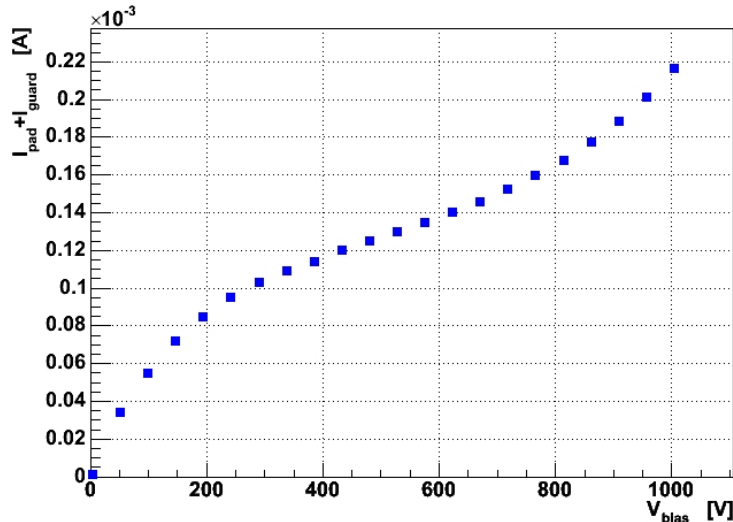


Figure 8: I-V characteristic of diode A1 after irradiation ( $2 \times 10^{14}$   $1\text{MeV } n_{eq} \text{ cm}^{-2}$ ) and annealing (152 min. at 80°C) up to 1000 V at 21.9°C.

## 2.2 Laser Test Setup

A test system based on a pulsed infrared laser was built at CERN in order to provide information on the signal generation for the electronic chip design. Current tests are limited to prototype diodes of 3 mm x 3mm. The laser system provides also an alternative possibility to determine the depletion voltage by measuring the total collected charge as function of the bias voltage. The amount of charge collected increases proportional to the depletion layer depth which is increasing with  $V^2$ . At full depletion the amount of charge collected remains constant.

A single mode class III Fabry-Perot InGaAs laser diode providing a laser light with a wavelength of 1060 nm corresponding to photon energy of 1.17 eV is used to illuminate the silicon diode. For this purpose, the Aluminum layer on the front-side of the sensor above the  $p^+$ -implant (see Figure 9) has to be removed to allow the light to penetrate into the Silicon. The circular opening on the test-diodes has a diameter of 2 mm. Choosing a photon energy just above the energy gap of Silicon at room temperature (1.12 eV) ensures uniform density of ionization along the beam path in the Si-sensor. The laser light with a wavelength of 1060 nm can penetrate  $\sim 890 \mu\text{m}$  into the silicon bulk [8].

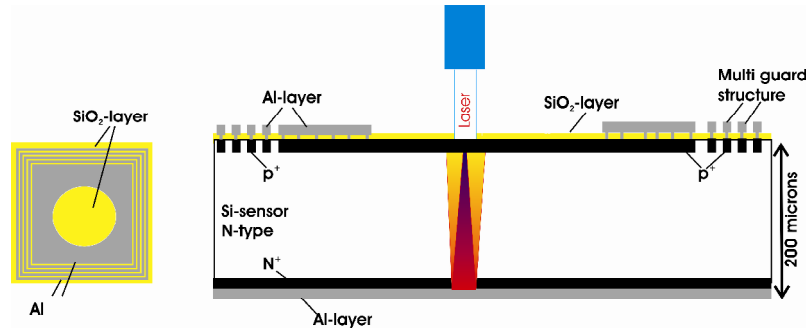


Figure 9: Schematic drawing of the light path in the silicon diode. The opening in the Al-layer on the front-side of the diode above the  $p^+$ -implant is shown to the left.

The laser is biased using an HP<sup>2</sup> 81112A 330 MHz Pulse/Pattern generator at a repetition rate of 1 kHz and the laser pulse can be made as short as 0.8 ns. The laser diode was pigtailed with a 3 m long single mode fibre, which is on the other end oriented perpendicular to the silicon sensor surface with a beam spot size of less than 10  $\mu\text{m}$  on the surface.

The bias voltage for the diode is provided with a Keithley power supply. The signal is extracted from the Si-diode from the pad via an Agilent MSA-0886 amplifier. A 22 nF capacitance in combination with a 10 k $\Omega$  resistor is applied in order to decouple the diode. The output of the amplifier is brought to a 1 GHz 9374M LeCroy oscilloscope which is used for data acquisition.

Figure 10 shows the registered laser pulse for different bias voltages measured on a non-irradiated diode. Figure 11 displays the signal area which is proportional to the collected charge as a function of the bias voltage. The depletion voltage is determined by fitting a

<sup>2</sup> Hewlett Packard, European Marketing Centre, P.O. Box 999, 1180 AZ Amstelveen, The Netherlands

$\sqrt{V}$  function to the first part of the curve and a line to the second part. The intersection determines the full depletion voltage  $V_{fd}$ .

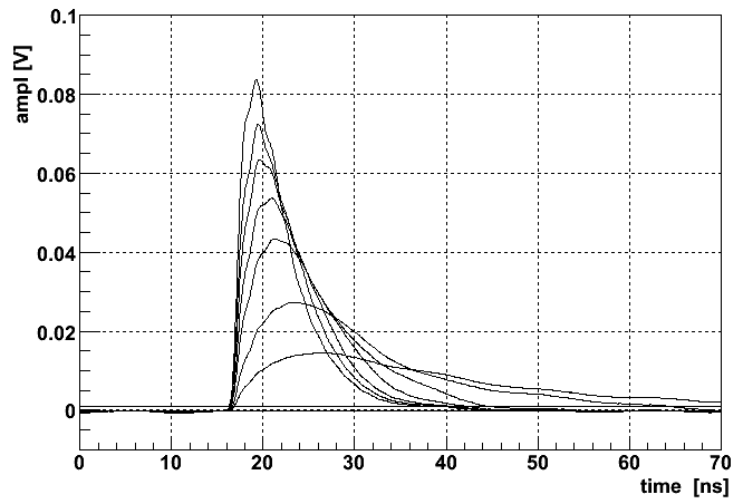


Figure 10: The signal pulse forms for different detector bias settings (20-300 V) at optimum pulse generator settings.

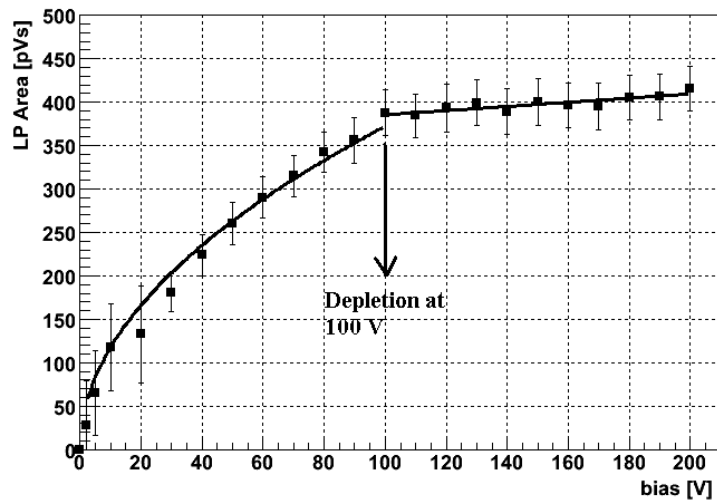


Figure 11: Registered pulse area as function of the bias voltage measured for diode B15 before annealing.

### 3 Irradiation and Annealing Results

Prior to irradiation all diodes have been tested measuring the C-V and I-V characteristics. The full depletion voltage  $V_{fd}$  before irradiation was found to be  $\sim 15V$ . One test diode has also been measured using the laser setup confirming the full depletion voltage determined by the C-V measurement. The typical leakage currents measured at 50V before irradiation were found to be 0.6 nA at  $20^{\circ}C$  after dicing and mounting on small PCBs.

After irradiation the diodes were initially stored inside a freezer at  $-27^{\circ}C$  until the radiation levels had sufficiently decreased. C-V and I-V measurements have been taken on the irradiated diodes before the first annealing step. During 2006 the laser setup was being constructed and all diodes that were irradiated in 2007 could also be measured with the laser prior to annealing.

Table 4 shows the list of measurements carried out after irradiation. Due to a problem in the setup in the chuck connection and therefore resulting in wrong current measurements, the measurements marked with (\*) will not be considered in the following analysis.

Diode	Size	Fluence [ $\times 10^{12}$ ]	C-V + I-V before annealing	Laser before annealing	Annealing	Laser after annealing
B2	3x3	1	yes *	-	yes*	no
B3	3x3	2	yes *	-	yes*	no
B4	3x3	10	yes *	-	yes*	no
A2	7x7	30	yes	-	yes	no
A1	7x7	200	yes	-	yes	no
846	3x3	3.49	yes *	-	yes*	no
847	3x3	5.92	yes *	-	yes*	no
848	3x3	8.4	yes *	-	yes*	no
849	3x3	25.1	yes	-	yes	no
B10	3x3	1.5	yes	-	yes	yes
B11	3x3	3	yes	yes	yes	yes
B12	3x3	5	yes	yes	yes	yes
B13	3x3	7	yes	yes	yes	yes
B14	3x3	15	yes	yes	yes	no
B15	3x3	100	yes	yes	yes	yes

Table 4: List of all measurements carried out after irradiation.

### 3.1 Leakage Current

Figure 12 shows the current density vs. voltage measured on four diodes after irradiation and before annealing at 80°C. The current values have been normalized to 20°C.

As due to setup limitations not on all diodes the guard and pad currents could be measured separately, in the following only the total currents are regarded. Figure 13 shows the total leakage current measured at 200V for all diodes plotted as function of the fluence. A line has been fitted to the data to obtain the damage constant  $\alpha$  at 20°C following

$$\Delta I_{Vol} = \alpha \cdot \phi_{eq} \quad \text{Eq. 3}$$

where  $\Delta I_{Vol}$  denotes the change in volume current and  $\phi_{eq}$  is the equivalent fluence in 1MeV  $n_{eq}/\text{cm}^2$  [6]. The damage constant  $\alpha$  at 20 °C obtained from the fit amounts to  $6.5 \times 10^{-17}$  A/cm which is in agreement with the expected values from literature ( $\alpha=4 \times 10^{-17}$  A/cm). The slightly higher value is accounted to the fact that the guard ring current is not separated in the measurements.

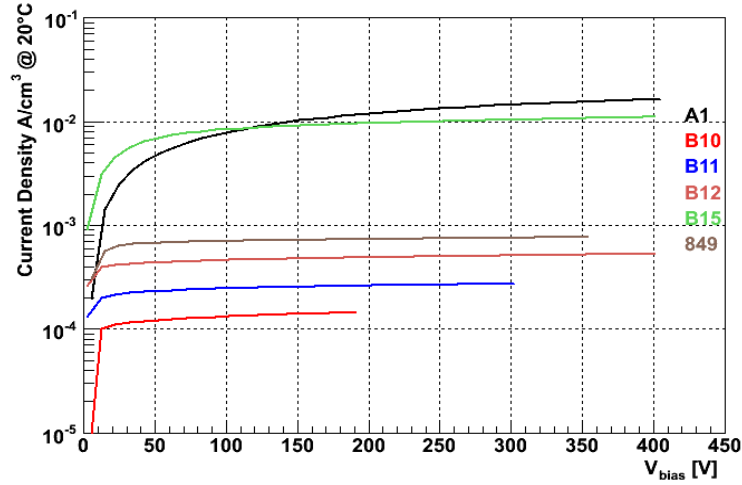


Figure 12: I-V characteristic measured on diodes after irradiation and before annealing. Values have been normalized to 20°C.

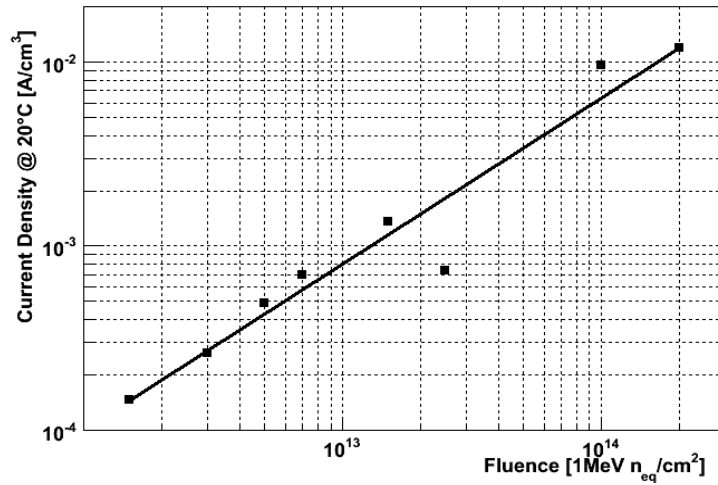


Figure 13: Total current at 200V normalized to 20°C and to unit surface as a function of the equivalent fluence.

Table 5 shows the expected leakage currents on the full size detector based on diode measurements, normalized to room temperature (RT) at 20°C and to the target operating temperature.

Diode	Fluence [1MeV n <sub>eq</sub> /cm <sup>2</sup> ]	Running days	Current @ 5°C [μA]	Current @ 20°C [μA]
A1	2 × 10 <sup>14</sup>	100	330	3900
B15	1 × 10 <sup>14</sup>	50	270	3100
B12	5 × 10 <sup>12</sup>	2.5	13	160
B11	3 × 10 <sup>12</sup>	1.5	7	90

Table 5: Leakage current of irradiated diodes, scaled to the full size of NA62 detector, for different fluences and the corresponding days of run. Currents have been measured at 200 V and at RT. They are here presented for two temperatures of the sensor (normalization to 5°C and 20°C using Eq. 2).

### 3.2 Depletion Voltage

At the same time as the I-V measurements were taken after irradiation also a C-V measurement was carried out to determine the full depletion voltage. C-V measurements

were carried out at least 2 different frequencies and in most cases at 3 frequencies as mentioned earlier. Figure 14 shows the full depletion voltage as determined from the C-V measurements after irradiation plotted as function of the equivalent fluence. The inversion appears to occur at around  $5 \times 10^{12}$   $1\text{MeV } n_{\text{eq}} \text{ cm}^{-2}$ . All measurements have been carried out after a storage time in a freezer at  $-27^\circ\text{C}$  of about 100 days.

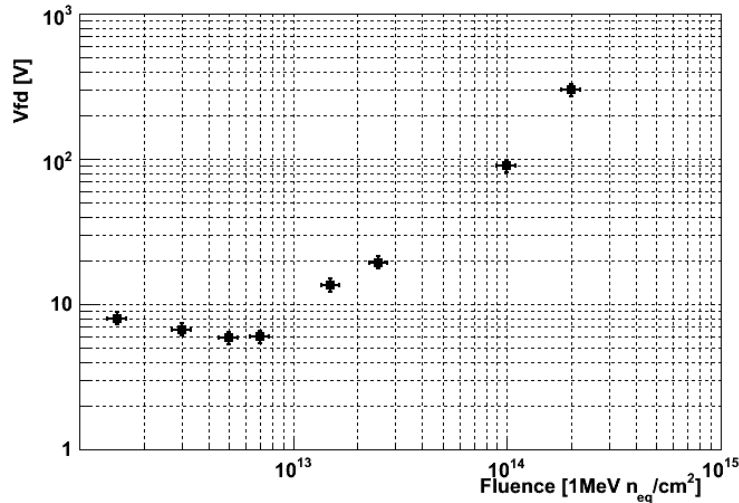


Figure 14: Full depletion voltage measured after irradiation as function of the fluence.

Following the recommendations of the ROSE collaboration the full depletion voltage was also determined after annealing of 4 minutes at  $80^\circ\text{C}$  [6] in order to remove all beneficial annealing. Figure 15 shows the results of the full depletion voltage measurement after 4 minutes at  $80^\circ\text{C}$  for the different diodes. An equivalent time of 4 minutes at  $80^\circ\text{C}$  corresponds to about 250 days at  $5^\circ\text{C}$  which would be more than one year of operation in the experiment at a realistic operating temperature. Figure 15 shows that the inversion point is around  $1 \times 10^{13}$   $1\text{MeV } n_{\text{eq}} \text{ cm}^{-2}$  which is in agreement with the results obtained by the ROSE collaboration.

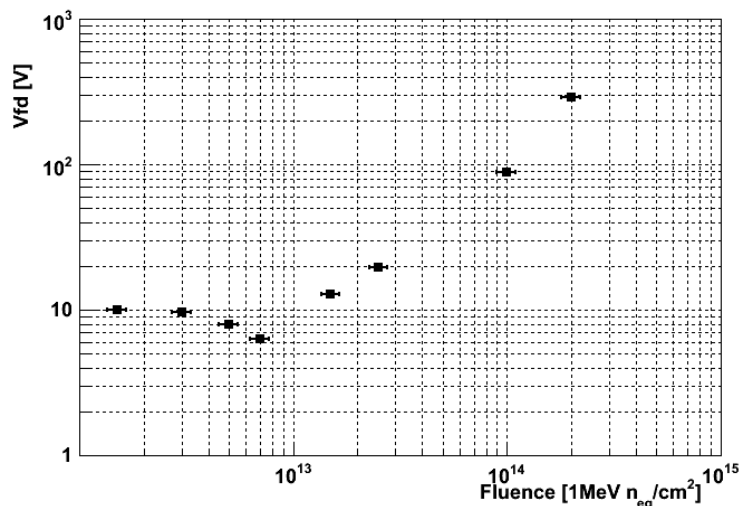


Figure 15: Full depletion voltage measured after irradiation and 4 minutes annealing at  $80^\circ\text{C}$ .

For the most recently irradiated diodes the full depletion voltage immediately after irradiation was also determined by using the laser setup.

Figure 16 shows  $V_{fd}$  measured with these two different methods for diodes B11 to B15. For all measurements the results obtained for  $V_{fd}$  with these two independent methods are in good agreement.

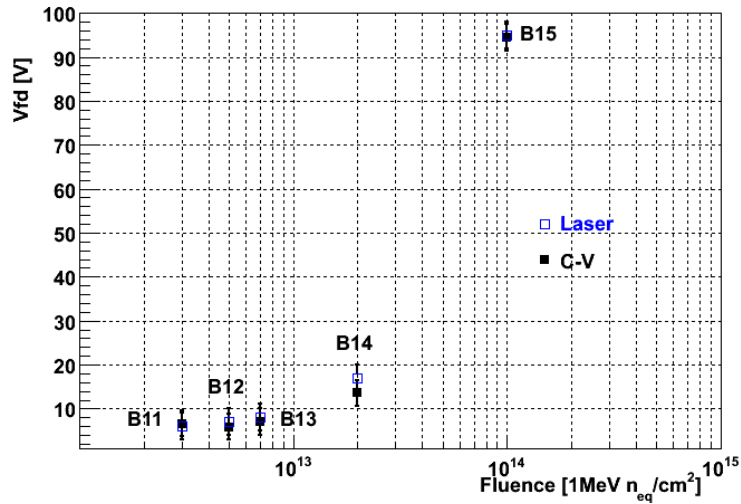


Figure 16: Comparison of the full depletion voltage determined by C-V measurements and by laser measurements for diodes B11-B15.

### 3.3 Annealing

All diodes underwent an annealing study which was carried out by heating the diodes at  $80^\circ\text{C}$  in an air convection oven for several time steps and measuring the I-V and C-V characteristics at all steps. The time intervals in the oven chosen were 2', 2', 4', 8', 8' and 16' and 60'. Figure 17 and Figure 18 show the leakage current, at the indicated voltages, versus annealing time for all diodes, normalized to equivalent time at  $5^\circ\text{C}$  following the Hamburg model [7].

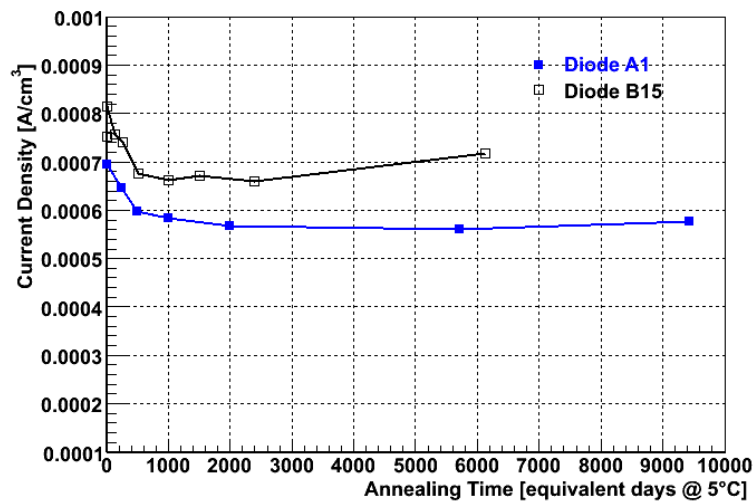


Figure 17: Total leakage current measured at different times of annealing for the diodes irradiated to the highest fluences.

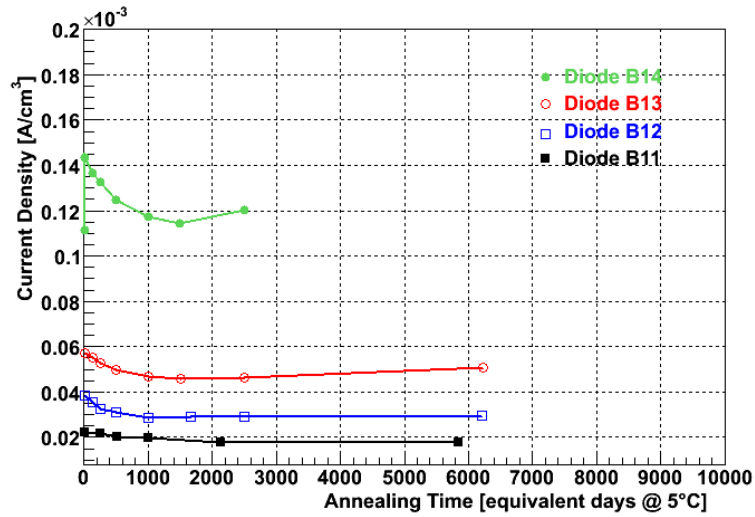


Figure 18: Total leakage current measured at different times of annealing for the diodes irradiated to lower fluences.

During the annealing the full depletion voltage was determined at every time step. Figure 19 and Figure 20 show the results of this measurement for all diodes tested.

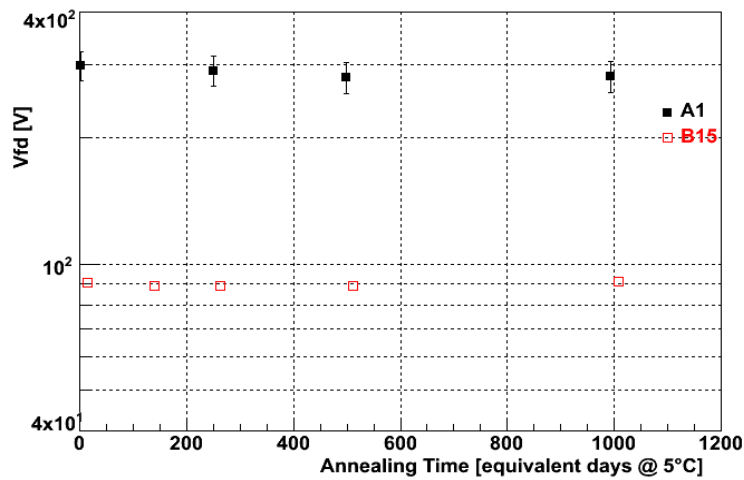


Figure 19:  $V_{fd}$  as a function of the annealing time for the diodes irradiated to the highest fluences.

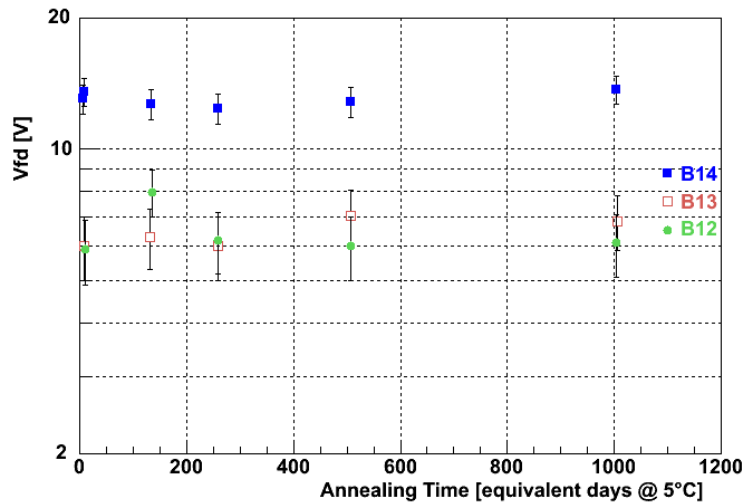


Figure 20:  $V_{fd}$  as a function of the annealing time for the diodes irradiated to lower fluences.

## Conclusions

The effects of radiation-induced damage to silicon sensors were investigated in view of using silicon pixel tracking detectors in the proposed NA62 experimental setup. Three planes of silicon pixel detectors with a pixel size of  $300\ \mu\text{m} \times 300\ \mu\text{m}$  will provide precise momentum and angular measurement of the initial kaon beam. The pixel detector will operate at high rate with almost 1 GHz/station.

The high rate operation of the GTK implies high radiation fluences to which the silicon detectors will be exposed. The intensity distribution of the beam will cause non-uniform irradiation of each GTK station, with a hot spot in the center of the plane. Fluences of up to  $2 \times 10^{14}\ \text{1MeV n}_{\text{eq}}\ \text{cm}^{-2}$  are expected during one year of operation (approximately 100 days) which are comparable to the fluences expected in the inner trackers of LHC experiments over 10 years.

A critical parameter in operating the GTK is the radiation induced leakage current of the relatively large sensor ( $60\ \text{mm} \times 27\ \text{mm}$ ). The leakage current can be limited by low temperature operation, which requires an efficient dissipation of thermal power from the detector and a good cooling system effective on the whole area of the device.

The measured leakage currents for the diodes irradiated to different fluences result in a damage constant of  $6.5 \times 10^{-17}\ \text{A/cm}$  at  $20^\circ\text{C}$  which is in agreement with literature. As can be seen in Table 5 an operating temperature of  $5^\circ\text{C}$  or less in any point of the GTK plane yields a leakage current of  $\sim 270\ \mu\text{A}$  for a full size module over an operating time of 50 days. Comparing the expected leakage currents for the diodes at  $20^\circ\text{C}$  this results in currents of  $3.3\ \text{mA/cm}^2$  for an operation time of approximately 50 days (diode B15), which will result in thermal runaway of the detector current. Thus efficient cooling is essential to allow as long as possible stable operation of each GTK module in the beam.

For a full operation time of one year (100 days) the maximum expected full depletion voltage for the fluence in the hot center of the beam is in the order of 300V (diode A1). An additional over-depletion voltage of up to 200V will be required to allow for sufficiently fast charge collection to fulfil the timing requirements of the experiment. The highly irradiated diodes have been all measured up to several hundred volts and in some cases up to 1000V to test the current stability at high voltages. A stable operation at around 500V seems to be possible with the current sensor design.

## Acknowledgments

The authors would like to express their gratitude to M. Glaser from the CERN PH/DT2 group for his invaluable help during the characterization and irradiation of the diodes. Special thanks are due to I. Mandic from the Jožef Stefan Institute in Ljubljana for the irradiation of diodes and to A. Rudge from Ohio State University for his essential help with the readout used in the laser setup. We are also indebted with I. McGill, F. Cossey-Puget and A. Guipet from the CERN wire bonding team. We thank ITC/IRST (Trento, Italy) for providing the diodes that were used in this work. The authors are very grateful to G. Stefanini/CERN for his constant support and help in preparing this note.

## References

- [1] CERN-SPSC-2005-013
- [2] M. Scarpa: The P326 Gigatracker, Nucl.Instrum.Meth.A566:127-129, 2006
- [3] M. Fiorini et al.: The P326 (NA48/3) Gigatracker: Requirements and design concept, Nucl.Instrum.Meth.A572:290-291, 2007
- [4] A. Kluge et al.: The Alice Silicon Pixel Detector, Proceedings of the 8<sup>th</sup> ICATPP, Como, Sept. 2003
- [5] C. Piemonte, Time response simulation of the NA48 silicon pixel detector, talk given in the Gigatracker working group, 2005  
<http://indico.cern.ch/materialDisplay.py?contribId=s1t4&materialId=0&confId=a057009>
- [6] Lindstroem et al, Radiation hard silicon detectors – developments by the RD48 (ROSE) collaboration, Nucl. Instr. And Meth. A 466 (2001)
- [7] Z. Li and H.W. Kraner, Studies of frequency dependant C-V characteristics of neutron irradiated p+-n silicon detectors. IEEE Trans. Nucl. Sci. 38:244-250, 1991
- [8] Vishay Telefunken: Application Note “Physics and Technology – Emitters”, page 3, Figure 64 <http://www.vishay.com/doc?80113> January 2008